

Storm Surge and Sea Level Rise Impacts on Avian Biodiversity by Functional Traits: Assessment Using Adaptive Ensemble Deep Learning Models

Liying Li, Marcos Zuzuarregui, Junwen Bai, Shoukun Sun, Yangkang Chen, Zhe Wang, Danial Fink

Abstract

Deep learning models have demonstrated their strong capability in identifying patterns in various areas, such as finance, medicine, and disaster forecasting. In this research, deep learning models were employed to detect species distribution patterns and map the impacts of storm surge and sea level rise on the Gulf's ecosystem biodiversity. This effort was built on an existing artificial intelligence (AI) technique, Deep Reasoning Neural Networks-Multi-variate Probit Models (DRNets-MVPM), and the species distribution model, Adaptive Spatial Temporal Ensemble Models (AdaSTEM). A suite of species and environmental data was synthesized to model two storm surge and sea level rise scenarios (Low and Intermediate-High). The deep learning approach was theoretically supported by both the biotic and abiotic niches of species, as modeled against 34 predictive variables for 332 species simultaneously. We found that deep learning models have superior prediction performance across species with well-documented data. Ensemble models have better stability and accuracy than single models at all levels, namely species-level, richness-level, and community-level. Species competition and synergies exhibited seasonal variation, with more competition during the summer and more synergies over the winter. Storm surge at low sea level rise will shift bird species inland and induce higher density of species in distribution areas near coastal areas, potentially intensifying species competition. In comparison, storm surges with intermediate-high sea level rise scenarios will shift species ranges eastward or westward, rather than inland. This research will inform adaptive and responsive conservation actions for conserving ecosystem biodiversity in the Gulf, facing environmental change challenges.

Keywords: Deep Learning, Species Distribution Models, Storm Surge, Sea Level Rise, Bird Species Occurrence

Introduction

Among the threats that climate change poses to ecosystems, sea level rise (SLR) has a devastating impact on coastal ecosystems. Historically, the wetland habitat along the northern Gulf of Mexico coast has been a shifting mosaic of changing elevation and salinity gradients, resulting in shifts in vegetation species and patterns that confine birds' nesting and breeding locations (Burger, 2017). Model projections of sea level rise over the next century and beyond may shift the northern Gulf of Mexico coastal environments into a new equilibrium regime (Donoghue, 2011). The northern Gulf of Mexico is located at the intersection of the Atlantic, Mississippi, Central, and Pacific Flyways, making it the heart of bird migration. Sea level rise (SLR) and climate change are projected to impact the Gulf's bird species assemblage (Burger, 2017). Many salt and brackish marshes may become permanently inundated due to SLR. Loss of wetlands and low-lying terrestrial ecosystems can make four out of five bird species lose their current habitat by 2025 (Klingbeil et al., 2021). Seawater intrusion into freshwater would alter the salinity gradient and the marsh vegetation, as well as the coastal hydrology, geomorphology, and nutrient structure

(Michener et al., 1997). Landward edges will advance into what are currently freshwater marshes, shrub swamps, and uplands, changing where birds can find a place to nest. The migration of the estuarine-freshwater transition zone will drive species either landwards or even to extinction with SLR, especially due to destructive extreme events.

Birds may not adapt to extreme events at the same level as to slow changes (Van De Pol et al., 2010), and more frequent hurricanes and storms with climate change, flood nests, eggs, and chicks, which is detrimental to reproductive success. Therefore, extreme events can render islands, beaches, or salt marshes unusable for breeding or foraging birds (Daniels et al., 1993). Previous studies already suggest that habitats and coastal birds' species assemblages will shift considerably over the coming decades in the Gulf of Mexico (Day et al., 2008; Forbes & Dunton, 2006; Greenberg et al., 2006). However, there are knowledge gaps regarding the long-term ecological impacts of SLR on species-level population changes for a wide range of avian species and relevant shifts in community composition. Existing methods exhibit significant uncertainty in bird population projections (Klingbeil et al., 2021), as well as a lack of information on species and community composition, which makes it challenging for conservation planning and prioritizing key sites for preservation under various SLR scenarios proposed by the IPCC (Pierce et al., 2018).

Successful avian biodiversity preservation also requires an understanding of birds' resiliencies to environmental changes across different functional groups. Censuses of birds in coastal marshes of Alabama and Mississippi found that coastal alterations, SLR, and landward changes in habitat and salinity will lead to population increases in Seaside Sparrows and Clapper Rails and decreases in Least Bittern (Rush et al., 2009)—the former two species nested in habitats with higher salinity than the Least Bitterns. The Gulf is the heart of 4 North American flyways, hosting semiaquatic birds, and all land birds have been reported on islands of the Gulf or crossing its waters. Approximately 44% of the reported species are aquatic, 27% are marine, and 29% are terrestrial (Gallardo et al., 2009). Species distribution modeling that only projects the responses of a few species cannot comprehensively reflect the responses of avian biodiversity to an ever-changing environment. Community-level modeling efforts, such as those described by Ovaskainen et al. (2017) and Warton et al. (2015), emphasize the importance of jointly modeling species occurrences to account for ecological interactions and shared responses to environmental change.

In recent years, deep learning has emerged as a powerful approach for modeling complex ecological phenomena, including species distribution models (SDMs) (Dinnage, 2024). Deep learning models are well-suited for extending to multi-output settings in Joint SDMs (Bai et al., 2020). Deep learning method shows an advantage over traditional joint species distribution models (SDMs) in terms of computation speed, capturing complex non-linear interspecific interactions (latent spaces) (D. Chen et al., 2016; Tang et al., 2018), and handling sparse data (Hirn et al., 2024) and multi-modal data with scalable computation (Chen, 2020). Multi-modal approaches offer flexibility in handling high-dimensional, nonlinear, and multimodal relationships (Suzuki et al., 2016), often observed in ecological data (Christin et al., 2019). Interpretability can be improved via embedding analysis, making complex models ecologically insightful. Building on this, Bai et al. (2020) introduced a deep generative framework for joint species distribution modeling, leveraging a popular deep learning architecture, variational autoencoders (Kingma & Welling, 2022).

We used deep reasoning neural networks (Chen et al., 2021) for the multivariate probit model (Lesaffre & Molenberghs, 1991) (DRNets-MVPM) to achieve the research objective of predicting storm surge impacts on avian biodiversity by different sea level rise scenarios and inform conservation actions. DRNets-MVPMs have been tested as suitable for predicting joint

species occurrences with better performance than some of the best joint SDMs recognized in the literature (Davis et al., 2023; Norberg et al., 2019). This model also bridges the gap that existing deep learning SDMs often fail to be probabilistic models (Dinnage, 2024). Probabilistic models are generally considered superior to deterministic models as ecological observations are zero-inflated and have incomplete detection. Species that are not detected can represent a low occurrence probability rather than absolute absence. Additionally, not all factors that impact species distribution can be observed, as real-world entities do not exist in a vacuum. Therefore, a probabilistic deep learning model provides flexibility for imperfect detections, enabling accurate predictions.

To handle spatial and temporal non-stationary bias and capture seasonal species dynamics, DRNets-MVPs were ensembled in the AdaSTEM framework (Fink et al., 2020) to predict species distribution with spatial and temporal sub-models. An identical static version of DRNets-MVPM was used to compare its performance with that of the adaptive dynamic approach, AdaSTEM DRNets-MVPM. A total of 332 species were modeled simultaneously against 34 predictive variables to predict storm surge impacts on bird species distribution under both Low (+0.2m from the c. 2000 mean sea level (MSL) by 2100) and Intermediate-High (+1.2m from MSL by 2100) sea level rise scenarios. Predictive variables include remote-sensing data, projected climate data, simulated storm surge data, and observation covariates. The outputs of species distribution were then merged with species functional traits and analyzed to determine how morphological features, foraging behavior, and migration patterns affect birds' resilience to storm surge impacts. This framework accommodates species-specific responses, interspecies dynamics, and climate-driven habitat shifts, offering a toolset for decision-makers to respond to environmental change proactively. This study presents a novel fusion of deep learning and ecological modeling, delivering critical insights for conservation planning and ecosystem management in the face of rising seas and intensifying coastal hazards.

Methods

Spatial and temporal ensemble model with AdaSTEM

AdaSTEM has been applied to a wide range of studies that assess how species distribution patterns change across space (Fink et al., 2023), time (Fink et al., 2020), and various anthropogenic (La Sorte et al., 2022) and environmental factors (Cohen et al., 2020). These models reveal significant improvements in capturing species' habitat preferences (Li et al., 2025) and migration patterns (Haas et al., 2022) compared to static models (Chen et al., 2024). The integration of temporal temporally dynamic factors (e.g., climate variability and migration stages) can forecast invasive species risk (Formoso-Freire et al., 2023), range shifts risks of migratory species (La Sorte et al., 2017), and species movement dynamics (Ruiz-Gutierrez et al., 2021), which traditional models often inadequately capture (Soriano-Redondo et al., 2019). Ensemble models that adapt to non-stationary spatiotemporal heterogeneity can also address temporal and spatial observation biases in citizen science data (Fink et al., 2010). More importantly, they improve prediction performance by avoiding overfitting across a large spatial scale (de Rivera et al., 2019).

Compared to static models, AdaSTEM has the advantages of predictive accuracy and computational efficiency (E. J. Ward et al., 2022). However, static models can perform well under certain data conditions, particularly when spatial coverage is limited or data are clumped (Redding et al., 2017). The accuracy gains in AdaSTEM benefit predictions for nomadic or range-expanding

species the most (Andrew & Fox, 2020). Ensemble and adaptive partitioning methods can be computationally intensive, but are suitable for computational parallelization (Chen, 2020), which reduces training time.

The StemFlow package (Chen et al., 2024) was acquired and modified to perform the AdaSTEM. The 10-year eBird observation data were first grouped into each of the 12 months based on the observation day of the year and then were partitioned by the modified StemFlow package into spatial boxes (Fink et al., 2020) that dynamically adapt to observation data densities across space (minimum 500 samples per box). The spatial boxes were also constrained to be no larger than 5° longitude \times 5° latitude and no smaller than 1° longitude \times 1° latitude by implementing forced splitting or aggregation, respectively. The number of spatial boxes varies across months and dynamically adjusts to the available observations for each month. The temporal dynamic is essential for predicting the seasonal dynamics of species movement (Andrew & Fox, 2020). The modified StemFlow code can be found in the code availability session.

Deep reasoning neural networks for the Multivariate Probit Model

Deep reasoning neural networks (Chen et al., 2021) for a multi-variate probit model is a deep probabilistic neural network for joint species distribution modeling (JSDM) (Norberg et al., 2019) that captures both species–environment relationships and interspecies dependencies (D. Chen et al., 2016). Coupling biotic and abiotic factors fills the gaps in the incomplete characterization of real-world scenarios of predation and competition, which also influence distribution, a factor that traditional algorithms frequently overlook. However, at the local scale, they include information about biotic variables (Barlett et al., 2024).

Environmental features are first passed through three fully connected layers of sizes 256, 512, and 512 for feature extraction, activated using ReLU functions and regularized with an L2 penalty with $1e^{-5}$ weight decay (Figure 1). The final layer of feature embedding outputs a species-specific mean vector μ , representing the species-specific environmental responses. To handle species correlations and uncertainty not explained by μ , a learned low-rank latent residual covariance structure was introduced in DRNets-MVPM. This residual structure is represented by a learnable square root matrix $\mathbf{B} \in R^{S \times Z}$, which models inter-species dependencies. By combining this residual structure with a diagonal identity matrix \mathbf{I} , parameterized by z_dim (number of independent variables: 20), the model ensures that the final covariance matrix is valid (positive semi-definite) (Zhang et al., 2020). This structure enables the model to capture biologically meaningful residual co-occurrence patterns, such as species that often co-occur together beyond what environmental variables alone can explain.

$$\Sigma = \mathbf{B}\mathbf{B}^T + \mathbf{I}$$

This approach is inspired by latent factor models commonly used in JSDMs (Warton et al., 2015; Hui et al., 2013). We scale (normalization process) the mean environmental embedding μ with the square root of the Σ diagonal to ensure the scale of the residual mean aligns with the scale of uncertainty encoded in the covariance matrix.

$$\bar{\mu} = \mu \odot \sqrt{diag(\Sigma)}$$

There are two key steps in estimating species presence probabilities from the latent variable samples of environmental embedding μ and species embedding Σ . One is sampling noise from a standard normal; the other is transforming it via the learned mean and covariance to get realistic samples (Kingma & Welling, 2013). Monte Carlo Sampling from a Multivariate Gaussian ($N(\bar{\mu}, \Sigma)$) was used for sampling from residuals, and the sigmoid function was used to retrieve the probability of occurrence from the latent variable matrix. Sigmoid function is a fast and stable alternative for computing the probability of occurrence Φ to the Cumulative Density Function (CDF), and it preserves differentiability, allowing backpropagation to pass through this probabilistic layer. The stochasticity of the model by treating embedding as a standard distribution incorporates uncertainty (via sampling). Approximated presence probability was used to enable efficient training by minimizing a composite loss including a negative log-likelihood, Marginal Cross-entropy loss, and L2 regularization. Models were trained using a 500-sample mini-batch and a maximum of 100 epochs. The learning rate is $1e^{-3}$, with a decay ratio of 0.5 and three decays. Detailed functional model representations can be found in Chen et al. (2016). The model code is provided in the Code Availability section.

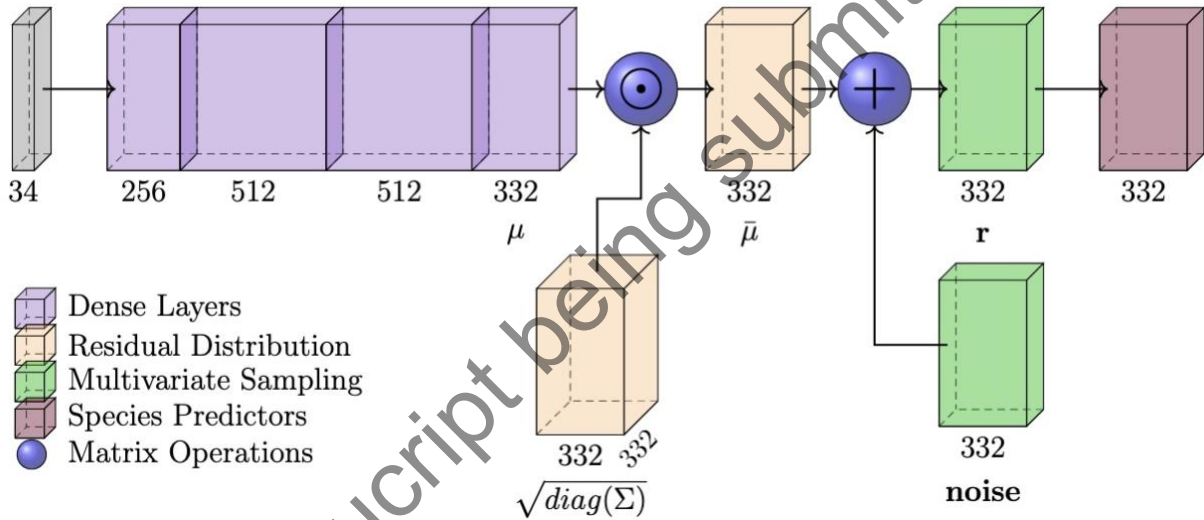


Figure 1. Diagram of DRNets-DVPM architecture of our residual, probabilistic network of learning environmental and species embedding (332 is the number of species, and 34 is the number of environmental and observation covariates)

Instead of modeling each binary response directly, the Multivariate Probit model (Lesaffre & Molenberghs, 1991) assumes that an underlying latent continuous variable determines each binary outcome. These latent variables are modeled jointly using a multivariate normal distribution, which enables correlations among the outcomes.

For range prediction, we converted the occurrence probability to presence/absence based on the Minimum Difference Threshold (MDT) criteria, which involves minimizing the difference between sensitivity (true positive) and specificity (true negative). MDT criteria have been approved as superior to other criteria, such as the 0.5T criteria (> 0.5 presence, < 0.5 absence) in predicting presence, particularly when the prevalence of presence is low (Jiménez-Valverde & Lobo, 2007). MDT criteria were implemented by looping through the threshold value from 0 to 1, searching for the threshold that minimizes the difference between the sensitivity and specificity metric for each species in each sub-model of the spatial boxes.

Species and environmental variables

eBird data (Sullivan et al., 2009) from 2015 to 2024 were acquired and merged for data augmentation. The data version used in this study was the 2025 eBird Reference Dataset. Checklists of all species were summarized into a table of all species observations, with each shared locality ID represented as a single row in the table, resulting in 408,338 entries (rows) including 448 species. Species with fewer than 100 occurrences across all entries and rows with only absence were removed, leaving 332 species with 404,058 data entries for subsequent model training.

Environmental predictors include both ancillary geographical information, such as digital elevation, orientation, and slope, as well as environmental variables, including temperature (Bio1 & Bio7), land use classes, biomass concentration, and chlorophyll concentration. Land cover is represented by the proportions of each land cover class in a 3×3 km area around each checklist.

The consideration of biomass and chlorophyll concentration underscores the importance of including the primary productivity of the ecosystem. We innovatively merge both land-based and oceanic environmental variables to create a consistent prediction that covers the coastline. Terrestrial biomass was obtained from the GEDI L4B Gridded Aboveground Biomass Density (Bubayah., 2023). SUOMI-NPP VIIRS Level-3 Mapped Particulate Organic Carbon was used for the Ocean biomass density approximation (NASA, 2022a). Mapped Particulate Organic Carbon in the ocean (units of mg C / m³) was superimposed on the GEDI L4B Gridded Aboveground Biomass Density. Similarly, the terrestrial leaf chlorophyll content for the year 2020 was acquired from the Global Leaf Chlorophyll Content Dataset (GLCC) derived from MERIS and OLCI Satellite Data (Qian et al., 2023). The ocean chlorophyll concentration was acquired from SUOMI-NPP VIIRS Level-3 Mapped Chlorophyll, Version 2022 (NASA, 2022b). A full description of the list of 28 environmental variable data used, along with the data sources, can be found in Supplementary Information 3.6. Observation covariates were included to control the observation bias in terms of observation duration, time of the day, day of the year, year of the observation, and travelling or stationary observation.

The difference in species resilience to climate change and sea level rise is analyzed by regressing predicted occurrence probability changes with different trait group features for each month across the whole year cycle with Ordinary Least Squares regression (OLS). Bird functional traits are acquired from the AVONET database (Tobias et al., 2022).

Storm surge by sea level rise scenarios

Climate change and sea level rise scenarios were created by modifying the historical prediction surface with replaced temperature and bathymetry digital elevation predictors under climate change. Projected temperatures were obtained from Bio-ORACLE (Assis et al., 2024) and WorldClim2 (Fick & Hijmans, 2017) for ocean and land, respectively, for both CMIP6 scenarios (SSP245 and SSP845) (O'Neill et al., 2016). SSP245 temperatures were used for low sea level rise scenarios, and SSP845 temperatures were used for intermediate high sea level rise scenarios. Bio7 is not directly available from Bio-ORACLE; therefore, we calculated the Bio7 mean temperature range for oceanic areas by using the difference between the maximum and minimum sea surface temperatures.

The simulated maximum of maximum (MOM) storm surge water surface elevation (Bilskie et al., 2016) was acquired and used to modify the historical bathymetry digital elevation. SWAN + ADCIRC (Simulating Waves Nearshore + ADvanced CIRCulation) was utilized in Bilskie et al. (2016) to predict water surface elevation with storm surge by different sea level rise scenarios. The mean sea level rise bathymetry elevation equals the historical mean bathymetry

elevation minus the predicted mean water surface elevation of inundation. The standard deviation of sea level rise bathymetry elevation equals the historical bathymetry elevation plus the standard deviation in predicted inundation water surface elevation, assuming the storm surge will increase the variation in water depths. We also modified the land cover class of water by revising the historical land cover classes of water based on whether the land is inundated. If land is inundated (the predicted mean water surface elevation of inundation is not zero), water cover is 1, and the other land cover classes are 0.

Results

Learned species-species and species-habitat relations

We pruned the species-environmental latent spaces based on the criterion of prediction precision, ensuring a value greater than 0.3, unless the species occurrence accuracy exceeded 0.97, to simplify the visualization of learned environment-species and species-species relations, also known as species embedding and environmental embedding, respectively. Each month, the list of species shortlisted is different. We plotted the interspecific embedding of the sampled species and their environmental (feature) embedding in Figures 2 and 3.

The correlation matrix in Figure 2 shows pairwise species relations. The species-species embedding (correlation values) has small variations across different pairs of species. Therefore, a Tahn-transform z-score normalization was applied to non-diagonal correlation values (correlation between different species). That is to apply tanh to bound values to $(-1, 1)$ smoothly after values were standardized using Z-score (mean 0, std 1) to make correlation values have a clear contrast and comparable across months.

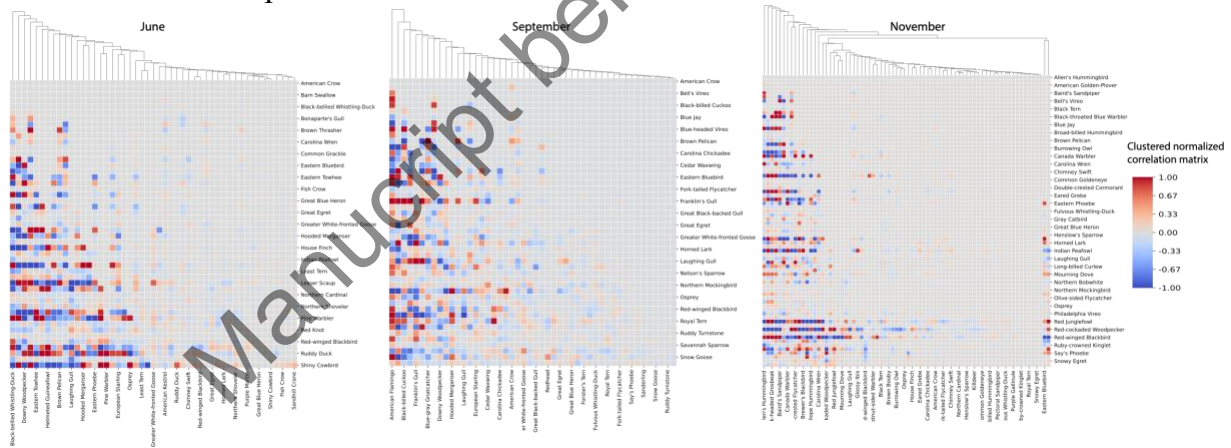


Figure 2. Clustered species-species correlation matrix (species embedding) for sampled bird species in different months in the Northern Gulf of Mexico

Environmental (feature) embedding of a species number by 512 dimensions was first reduced to 2D dimensions using t-SNE (Van Der Maaten & Hinton, 2008) and plotted in clusters based on pairwise dissimilarities (Figure 3). T-SNE is a nonlinear method that maps high-dimensional data into 2D or 3D using a t-distribution. If two points are close together in high-dimensional feature embedding space, they will be placed close to each other in Figure 3 using Kullback–Leibler (KL) divergence. Figure 3 illustrates the pairwise similarities among all sampled species within a month. In June, as species have relatively higher competition than in

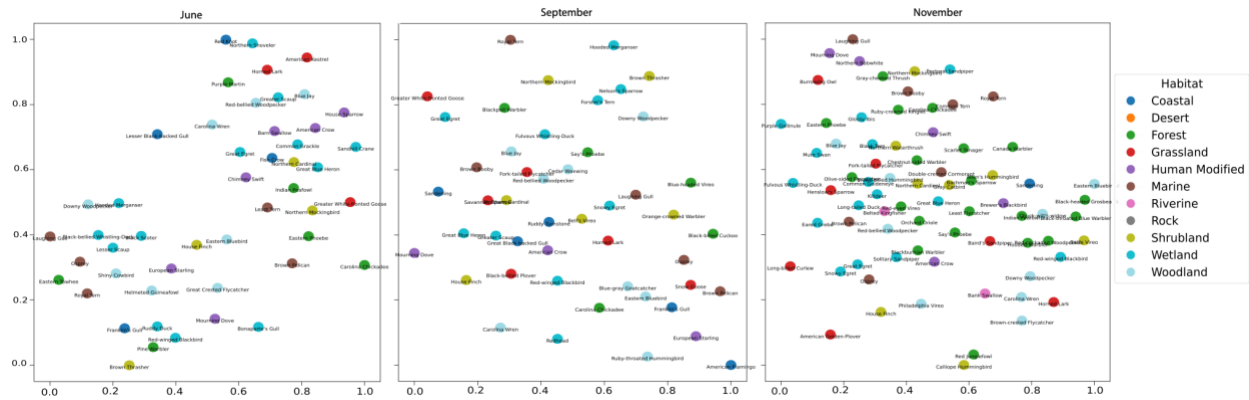


Figure 3. Clustered species-environment correlation (feature embedding) after t -SNE dimensions reduction for sampled bird species in different months in the Northern Gulf of Mexico

Storm surge impacts on the occurrence probability and range

If the historical occurrence probability of a species at a location is less than 1%, we set the occurrence probability to NA to avoid infinitely large proportional change results. We selected the species without NA values in probability change across the study area and plotted them in spatial maps (Figure 4a and 4b; additional species occurrence probability change maps are available in the data availability repository). Figure 4 shows the storm surge impacts on Laughing Gull, Great Egret, and Osprey in species occurrence probability if storm surge occurs in a certain season. Figure 4a has a low-level sea level rise, and Figure 4b shows an intermediate-high-level sea level rise. When the sea level rises are at a low-level, the Laughing Gull chooses to shift inland. If the storm surge had happened later in the year, in November, it would have had a higher impact on the occurrence of laughing Gulls than if it had happened in June. For the Great Egret, however, the impacts of seasonality are the opposite. If a storm surge had occurred in June, the occurrence probability would have been reduced by more than 50% in both coastal and inland areas. If it had happened in November, the impacts would have been minimal compared to other seasons. The effects on Osprey are similar to those of the Laughing Gull, in that winter storm surge has a higher reduction in occurrence probability. Even inland areas in Louisiana that were not impacted by simulated storm surge showed a pronounced decrease, as represented in the red map units.

When sea level rise is at an intermediate-high level, all three species exhibit different migration patterns to escape the disasters compared to the low-level scenarios (Figure 4b). Species shift either eastward (Laughing Gull and Great Egret) or westward (Osprey). The most vulnerable season for Laughing Gull and Great Egret is Summer, and for Osprey is Winter, in November. The most resilient season for Laughing Gull is Fall, for Great Egret is Winter, and lastly for Osprey is Summer.

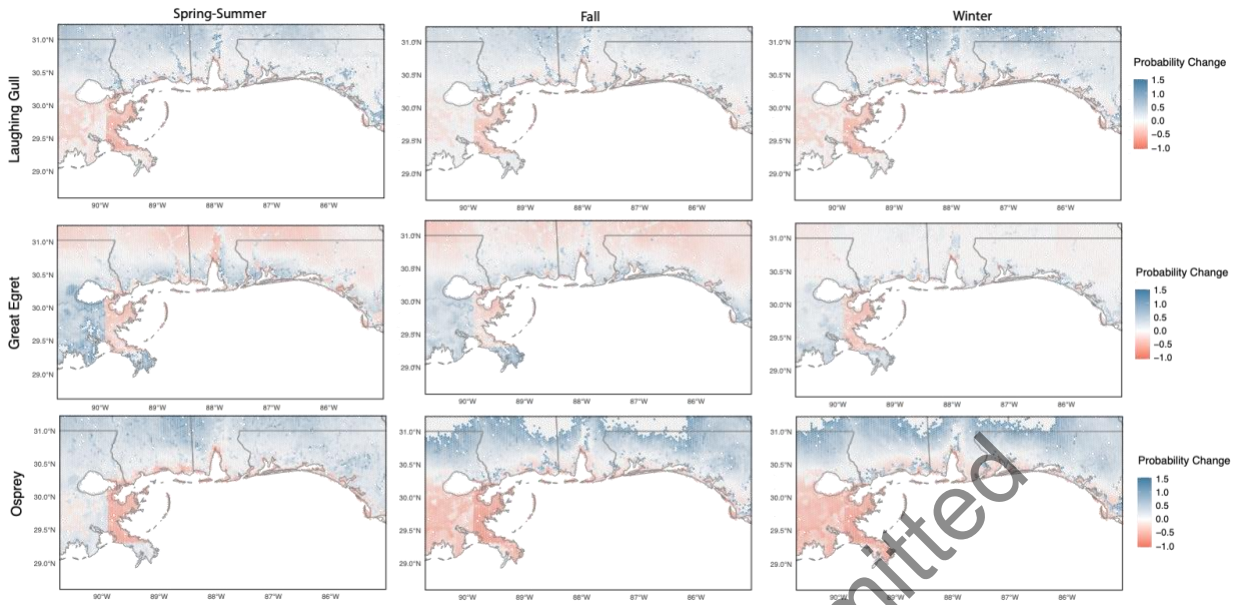


Figure 4a. Species occurrence probability change impacted by storm surge in different seasons at low-level sea level rise

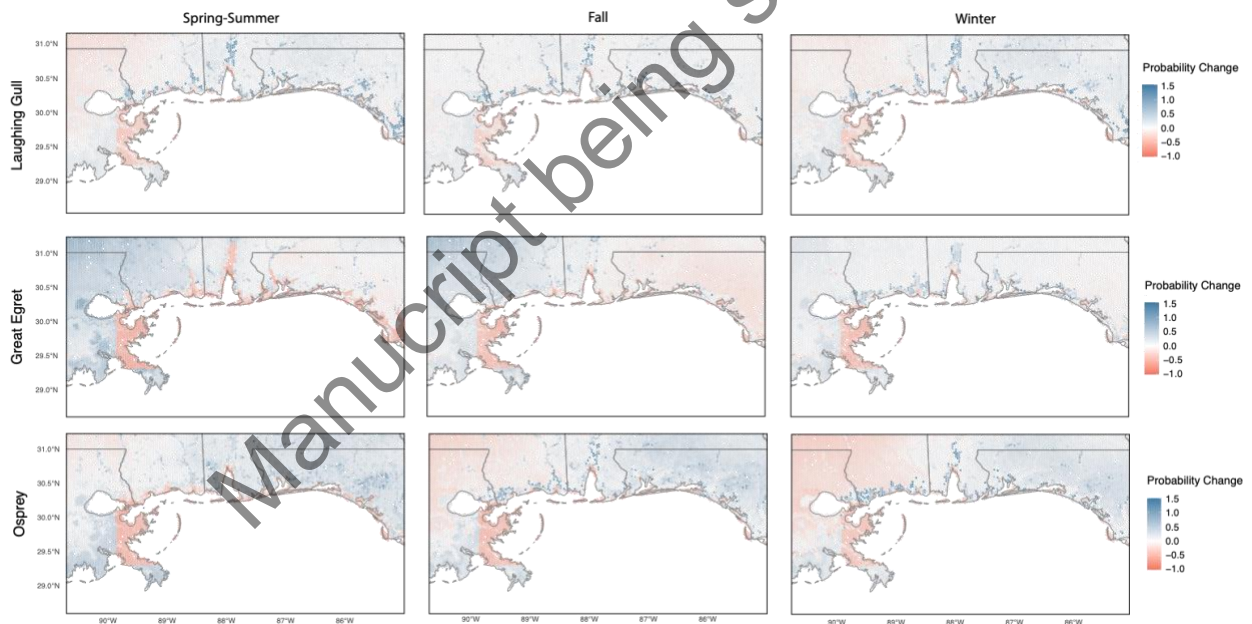


Figure 4b. Species occurrence probability change impacted by storm surge in different seasons at an intermediate-high level of sea level rise

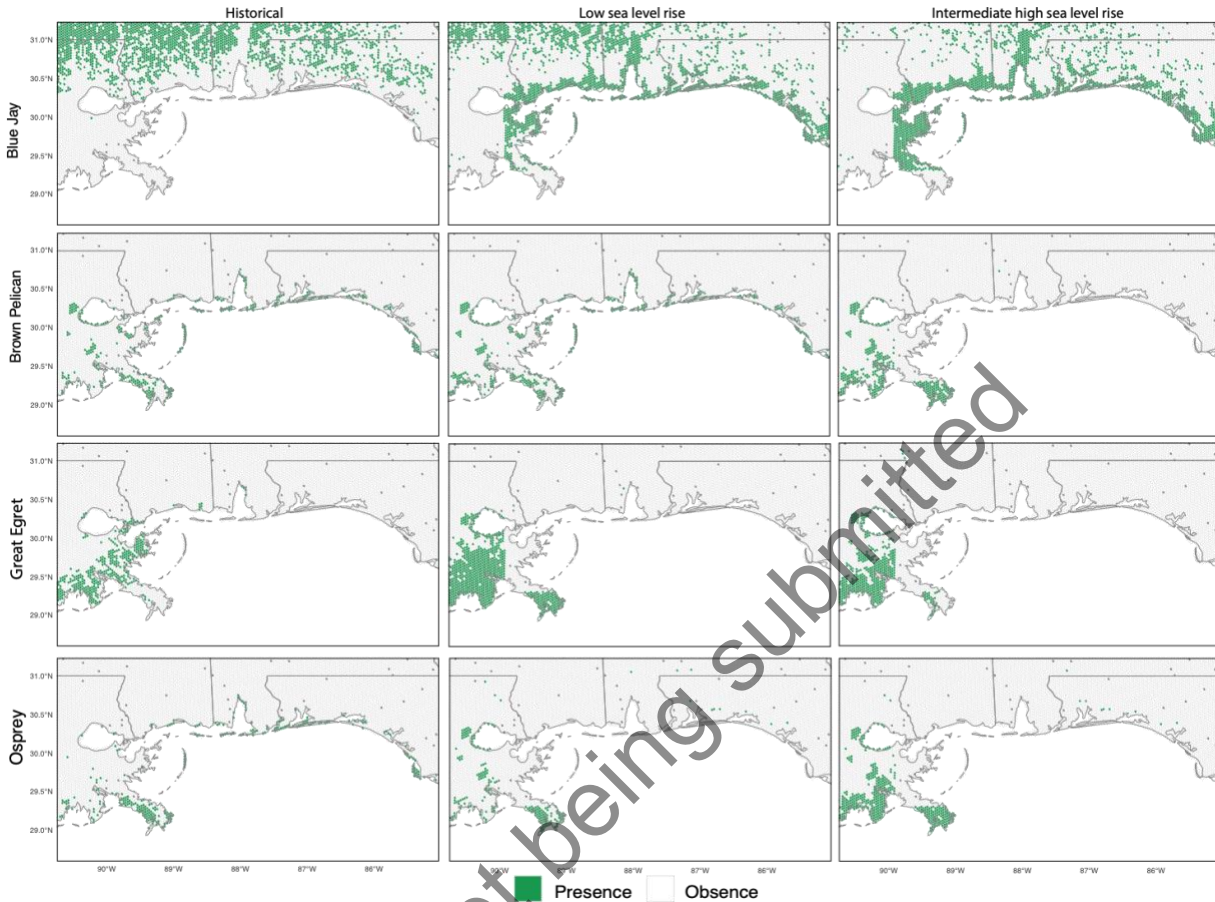


Figure 5. Species range shifts with different sea level rise scenarios, from historical, low-level sea level rise to intermediate-high level sea level rise, from left to right

Based on species occurrence probability, we used the MDT criteria discussed in the method section to convert occurrence probability into the presence or absence of species. Species range maps were plotted in Figure 5. The Great Egret and Osprey were kept in this figure to compare with the probability plots in Figure 4. The Laughing Gull was excluded because it has a similar pattern to the Osprey in the range map shifts. We also included two other species that have very distinct morphological features and are therefore widely recognized and easily observed to illustrate examples of different range shift patterns with good-quality predictions, as supported by a high observation rate. As a result, we observed a very interesting migration pattern of Blue Jays, flying from inland to flooded areas. Brown Pelican range didn't shift as apparently as other species in the low sea level rise scenario. If sea level rise increases with severity, Brown Pelicans will be wiped out across the Gulf coastline in Mississippi, Alabama, and Florida. They were driven to the Louisiana coast and inland areas that were not impacted by the simulated storm surge in this study (the simulated storm surge boundary is provided in Supplementary Information S1). The same range shift pattern can be observed in the Great Egret and the Osprey. However, the coastal Great Egret and Osprey are less resilient than the Brown Pelican; therefore, even under the low sea level rise scenario, their range was eliminated from the coastlines of Mississippi, Alabama, and Florida. Particularly, in the intermediate-high sea level rise scenario, Great Egrets were no longer observed in the storm surge-impacted area.

Species resilience to storm surge impacts by functional traits

After examining the occurrence and range shift patterns of individual species, we concatenated the predicted storm surge impact on species occurrence probability with the birds' trait features. The resilience of species to storm surge changes across functional trait groups was investigated and plotted using OLS regression, as described in the method section (Figure 6). If the coefficient is below zero, the further away from zero, the less resilient the trait group is to storm surge. The absolute value of the coefficient represents how much smaller the change in occurrence probability is than the mean. For example, if the mean occurrence probability changes by 0.1, the forest bird occurrence probability changes by -0.1 (0.1-0.2). If the coefficient value is above zero, the further away from zero, the more resilient the trait group is to storm surge. Figure 6 shows ordered trait groups from less resilient to more resilient from left to right for each trait category.

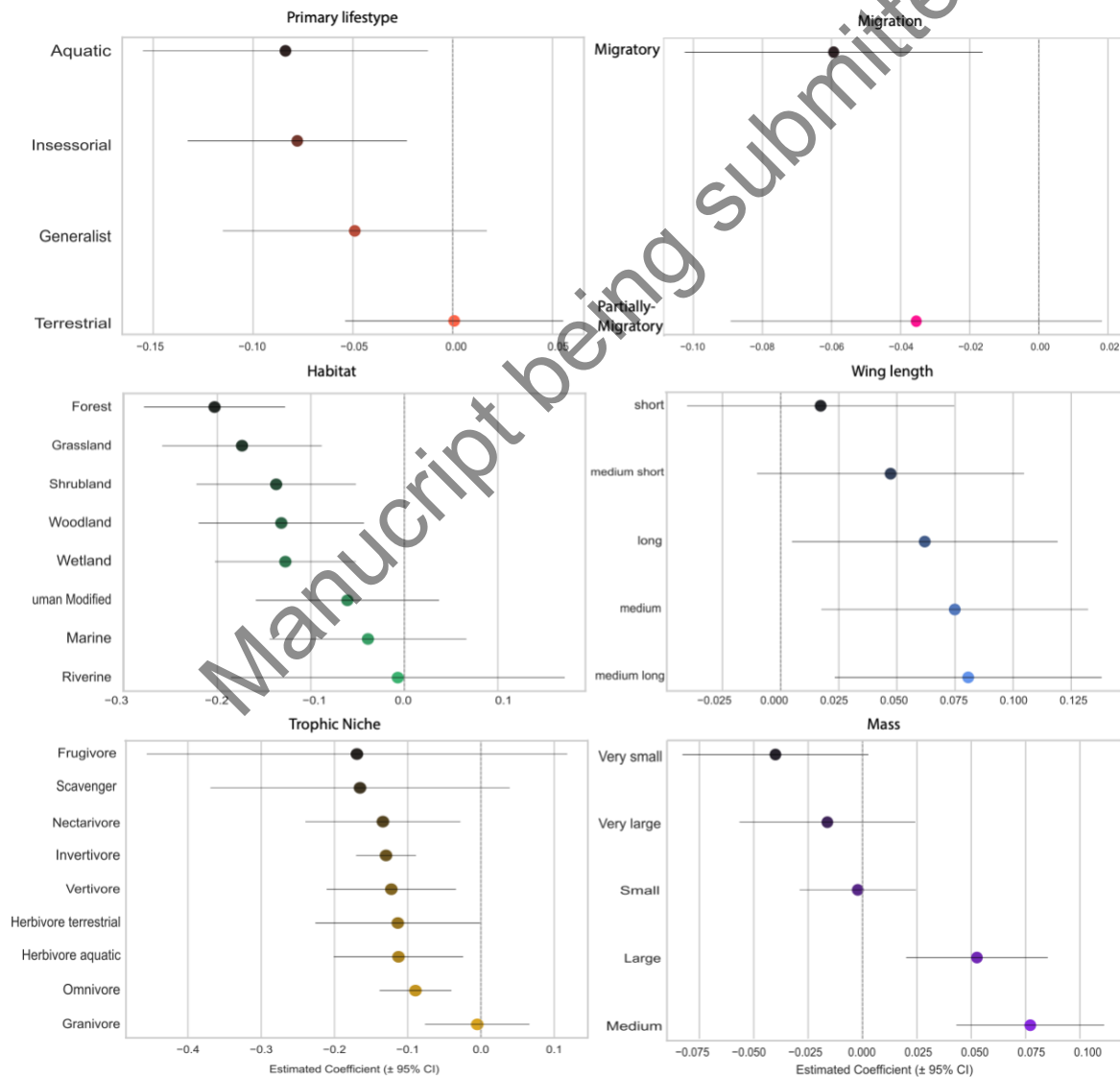


Figure 6. Effects of trait groups on species resilience to storm surge impacts in September in the intermediate-high-level sea level rise scenario, represented by OLS regression coefficients

For a continuous trait category, trait values were categorized into 5 groups based on quantiles, as shown in the plot for the Mass and Wing Length traits. Overall, a partially migratory bird is more resilient than a migratory bird. Medium-sized birds with medium-long wings are most resilient among different body weight and wing length groups. Understandably, this group of birds has the capacity to move a far distance faster than short-wing birds. At the same time, medium-sized body weight can allow them to travel with sufficient energy storage, while they are not as picky eaters as large-sized birds. As shown in the trophic niche trait category, the Frugivore is least resilient to storm surge, as they rely on fruits and plants that can be easily destroyed by the storm surge and may be hard to find in a different environment after escaping the impacted areas. Forest birds are the least resilient in storm surge (Figure 6), as forest habitat is slower to recover from devastating disasters than other habitats. The closer to the coast and water, the more vulnerable the species is to storm surge, as shown in the Primary lifestyle

Ensemble model performance evaluation

At the species level, AdaSTEM DRNets-MVPMs have higher F1 scores than static DRNets-MVPMs (Figure 7, full description of metrics can be found in Supplementary Information S2).

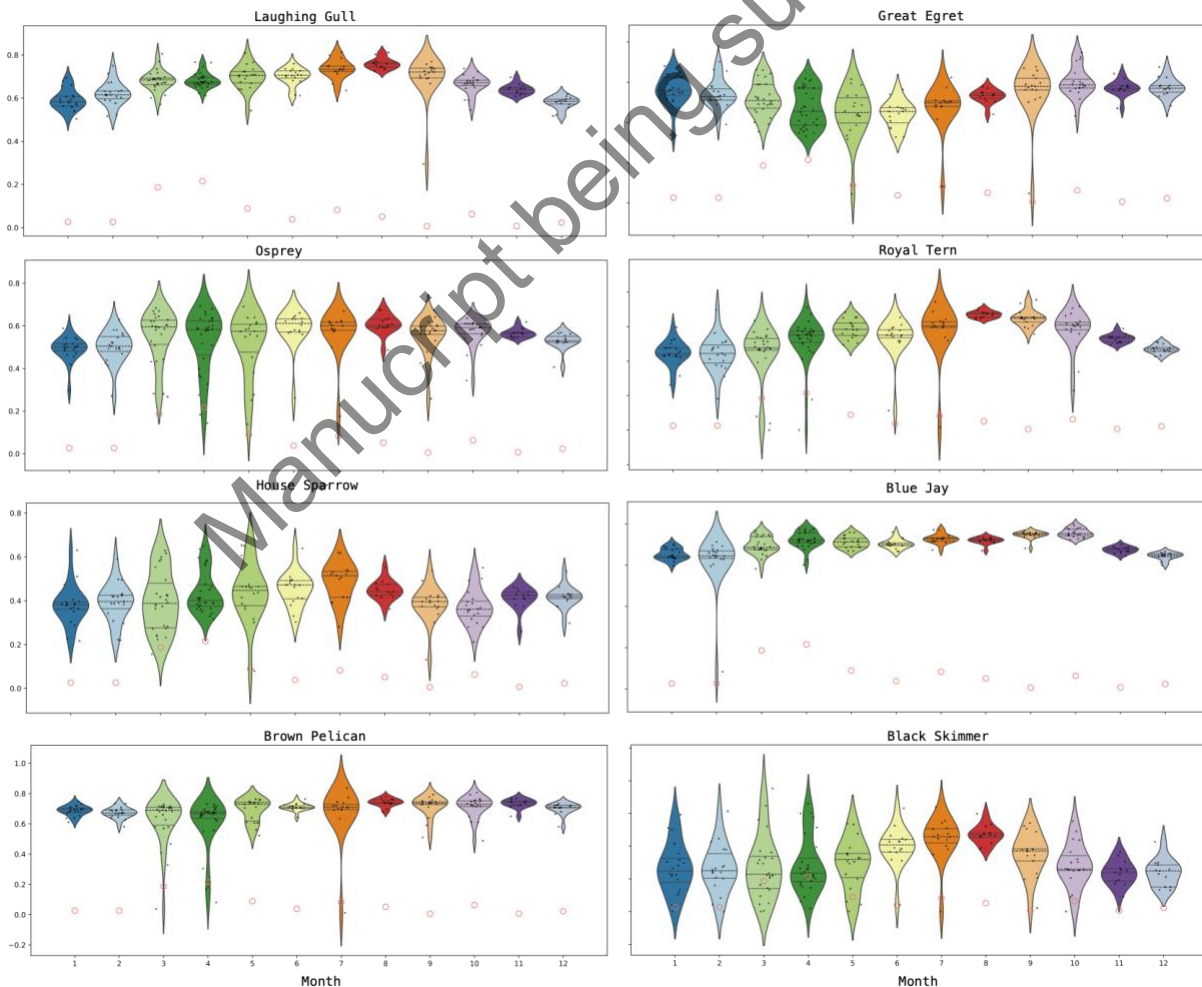


Figure 8. Examples of AdaSTEM DRNets-MVPM and static DRNets-MVPM F1 scores by species for predicting species presence/absence across 12 months of the year (black solid dots and violins represent the performance of AdaSTEM sub-models, and red hollow dots represent F1 score of the static model)

Additionally, AdaSTEM models have seasonal trending F1 scores, while the static model doesn't. The model has a better score in the summer for Laughing Gull, Royal Tern, and Black Skimmer, which are highly migratory and display strong seasonal habitat preferences. Blue Jays and Brown Pelicans showed less seasonal variation in model performance than other species. AdaSTEM DRNets-MVPMs captures timely appearances and environmental cues, leading to better precision and recall—and thus a higher F1 score when species are more abundant. Species like Laughing Gull, Royal Tern, and Black Skimmer shift in distribution and become more abundant during the summer breeding season. This leads to higher F1 scores.

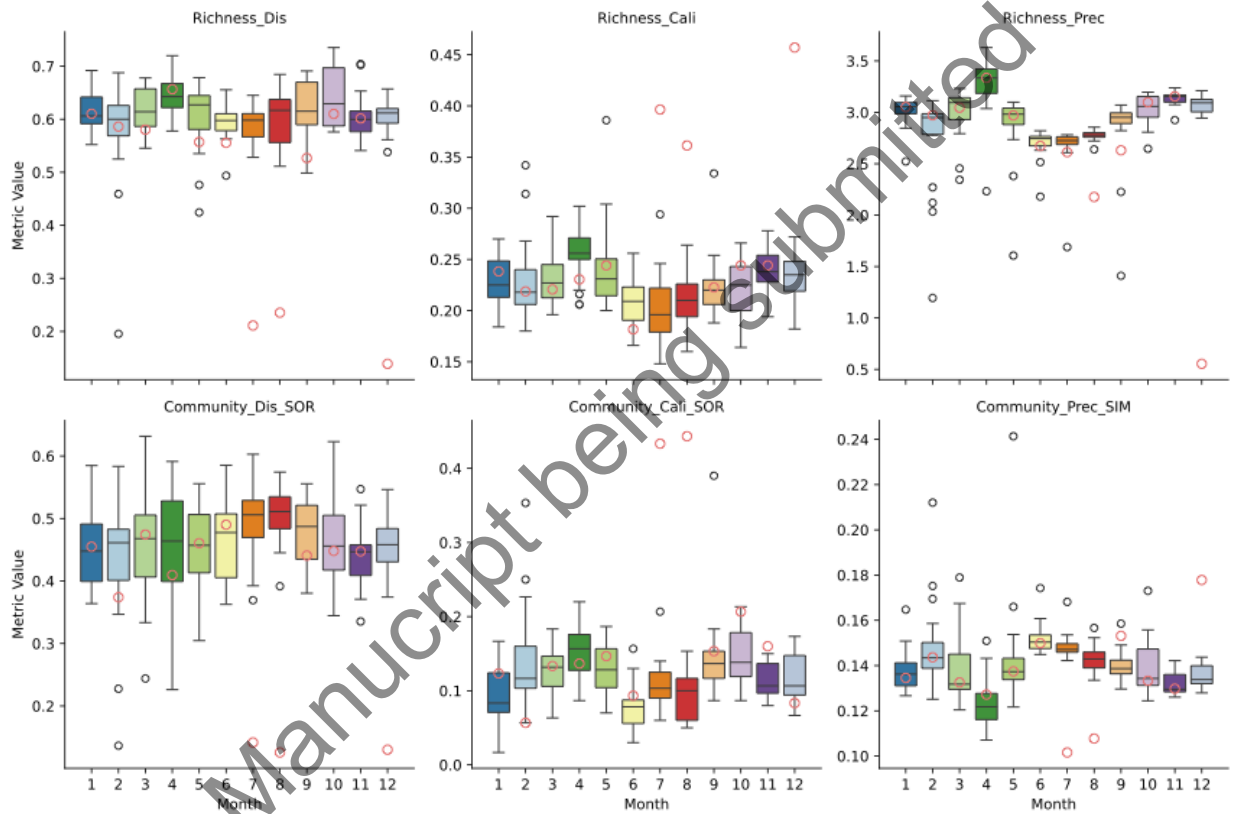


Figure 9. AdaSTEM DRNets-MVPM and static DRNets-MVPM richness and community level prediction performances for predicting species presence/absence across 12 months of the year (box plots represent the mean, quantile, and distribution of AdaSTEM sub-models metrics, and red hollow dots represent the static model metrics)

On the other hand, the Blue Jay and Brown Pelican exhibit more stable, year-round distributions, with less dramatic seasonal movement. AdaSTEM DRNets-MVPM achieved a better F1 score for Great Egrets in the winter, while the osprey was predicted more accurately in the spring. The Great Egret tends to migrate southward in winter to the Gulf coast and warmer wetland habitats. More observation led to AdaSTEM's adjustment to these season-specific habitat

preferences. However, a static model can't identify wintering grounds; therefore, it doesn't show a higher F1 score in the Winter.

Ospreys are long-distance migrants that return to breeding areas in spring, often near freshwater bodies with abundant fish. Their spring arrival creates this distinct seasonal signal in model performance, with better F1 scores generated by more observations, which AdaSTEM can leverage to refine predictions.

At the richness and community level, AdaSTEM DRNets-MVPMs consistently outperform static models by capturing seasonal and spatial dynamics in avian biodiversity (Figure 9). While calibration generally improves, a few outliers in richness and community calibration in the summer reflect challenges in modeling highly variable communities, caused by migration timing variations across space, and the observation of rare species with variable detection rates across different spaces covered by separate sub-models in AdaSTEM.

Conclusion

Coastal ecosystems face intensifying threats from climate change, yet conservation efforts are often constrained by limited foresight into how biodiversity will respond. This research advances the integration of deep learning into ecological forecasting by developing an ecologically informed and computationally scalable framework to model the impacts of storm surge and sea level rise on coastal biodiversity. By combining Deep Reasoning Neural Networks–Multivariate Probit Models (DRNets-MVPM) with Adaptive Spatiotemporal Ensemble Models (AdaSTEM), we produced high-resolution species occurrence predictions for 332 bird species across diverse spatial and environmental gradients using adaptive ensemble learning of deep neural networks. The resulting model captures both species-specific and community-wide ecological responses with improved accuracy, stability, and calibration compared to traditional static models.

The impact assessment using adaptive ensembled DRNet-MVPM accounts for seasonal dynamics in species interactions—highlighting competitive pressures in summer and greater ecological synergy in winter—and reveals differential redistribution patterns under distinct climate scenarios. Inland compression of species under low sea level rise, and east–west range shifts under Intermediate-high scenarios, demonstrate the model's ability to resolve complex climate–biodiversity relationships at multiple ecological levels.

Critically, it was revealed that species' functional traits strongly modulate their resilience to storm surge. Using regression-based trait analysis, we identify that partially migratory birds, medium-sized birds with medium to long wings, and generalist foragers are among the most resilient groups. In contrast, frugivores, forest-dependent species, and those with coastal or aquatic primary lifestyles are particularly vulnerable. This reflects a combination of mobility, energy demands, dietary flexibility, and the potential for habitat recovery. By connecting predicted range shifts with ecological traits, our model offers a mechanistic lens into species' resiliencies to climate-induced disturbances as constrained by their life-history strategies.

These findings offer a significant methodological advancement, demonstrating that deep learning can be ecologically interpretable, while scaling effectively across taxa, regions, and environmental gradients. Beyond methodological innovation, this work provides a practical tool for informing proactive and adaptive conservation strategies in coastal ecosystems. By forecasting how sea level rise and storm surge may reshape species distributions, alter community structures, and compress ecological niches, our approach equips decision-makers with early warnings about

regions and species at greatest risk under different climate futures. As sea level rise and extreme weather continue to reshape ecosystems globally, scalable AI-powered frameworks like ours will be vital for aligning ecological science with climate resilience and long-term conservation planning.

Data Availability

Data will be stored on Dryad

Code Availability

Code will be shared on ZENODO

References

- Andrew, M. E., & Fox, E. (2020). Modelling species distributions in dynamic landscapes: The importance of the temporal dimension. *Journal of Biogeography*, 47(7), 1510–1529. <https://doi.org/10.1111/jbi.13832>
- Bai, J., Kong, S., & Gomes, C. (2020). *Disentangled Variational Autoencoder based Multi-Label Classification with Covariance-Aware Multivariate Probit Model*. <https://doi.org/10.24963/ijcai.2020/595>
- Barlett, T. R., Laguna, M. F., Abramson, G., Monjeau, A., & Martin, G. (2024). A new distributional model coupling environmental and biotic factors. *Ecological Modelling*, 489. <https://doi.org/10.1016/j.ecolmodel.2023.110610>
- Bilskie, M. V., Hagen, S. C., Alizad, K., Medeiros, S. C., Passeri, D. L., Needham, H. F., & Cox, A. (2016). Dynamic simulation and numerical analysis of hurricane storm surge under sea level rise with geomorphologic changes along the northern Gulf of Mexico. *Earth's Future*, 4(5), 177–193. <https://doi.org/10.1002/2015EF000347>
- Burger, J. (2017). Avian Resources of the Northern Gulf of Mexico. In C. H. Ward (Ed.), *Habitats and Biota of the Gulf of Mexico: Before the Deepwater Horizon Oil Spill: Volume 2: Fish Resources, Fisheries, Sea Turtles, Avian Resources, Marine Mammals, Diseases and Mortalities* (pp. 1353–1488). Springer New York. https://doi.org/10.1007/978-1-4939-3456-0_4
- Chen, D. (2020). *DMVP-DRNets/eBird_entire at v1.0 · gomes-lab/DMVP-DRNets*. https://github.com/gomes-lab/DMVP-DRNets/tree/v1.0/eBird_entire
- Chen, D., Bai, Y., Ament, S., Zhao, W., Guevarra, D., Zhou, L., Selman, B., van Dover, R. B., Gregoire, J. M., & Gomes, C. P. (2021). *Automating Crystal-Structure Phase Mapping: Combining Deep Learning with Constraint Reasoning*. <http://arxiv.org/abs/2108.09523>
- Chen, D., Xue, Y., Chen, S., Fink, D., & Gomes, C. (2016). *Deep Multi-Species Embedding*. <https://doi.org/https://doi.org/10.48550/arXiv.1609.09353>
- Chen, Y., Gu, Z., & Zhan, X. (2024). stemflow: A Python Package for Adaptive Spatio-Temporal Exploratory Model. *Journal of Open Source Software*, 9(94), 6158. <https://doi.org/10.21105/joss.06158>
- Christin, S., Hervet, É., & Lecomte, N. (2019). Applications for deep learning in ecology. In *Methods in Ecology and Evolution* (Vol. 10, Issue 10, pp. 1632–1644). British Ecological Society. <https://doi.org/10.1111/2041-210X.13256>
- Cohen, J. M., Fink, D., & Zuckerberg, B. (2020). Avian responses to extreme weather across functional traits and temporal scales. *Global Change Biology*, 26(8), 4240–4250. <https://doi.org/10.1111/gcb.15133>

- Daniels, R. C., White, T. W., & Chapman, K. K. (1993). Sea-level rise: Destruction of threatened and endangered species habitat in South Carolina. *Environmental Management*, 17(3), 373–385. <https://doi.org/10.1007/BF02394680>
- Davis, C. L., Bai, Y., Chen, D., Robinson, O., Ruiz-Gutierrez, V., Gomes, C. P., & Fink, D. (2023). Deep learning with citizen science data enables estimation of species diversity and composition at continental extents. *Ecology*, 104(12). <https://doi.org/10.1002/ecy.4175>
- Day, J. W., Christian, R. R., Boesch, D. M., Yáñez-Arancibia, A., Morris, J., Twilley, R. R., Naylor, L., Schaffner, L., & Stevenson, C. (2008). Consequences of Climate Change on the Ecogeomorphology of Coastal Wetlands. *Estuaries and Coasts*, 31(3), 477–491. <https://doi.org/10.1007/s12237-008-9047-6>
- de Rivera, O. R., Blangiardo, M., López-Quílez, A., & Martín-Sanz, I. (2019). Species distribution modelling through Bayesian hierarchical approach. *Theoretical Ecology*, 12(1), 49–59. <https://doi.org/10.1007/s12080-018-0387-y>
- Dinnage, R. (2024). *NicheFlow: Towards a foundation model for Species Distribution Modelling*. <https://doi.org/10.1101/2024.10.15.618541>
- Donoghue, J. F. (2011). Sea level history of the northern Gulf of Mexico coast and sea level rise scenarios for the near future. *Climatic Change*, 107(1), 17–33. <https://doi.org/10.1007/s10584-011-0077-x>
- Fink, D., Auer, T., Johnston, A., Ruiz-Gutierrez, V., Hochachka, W. M., & Kelling, S. (2020). Modeling avian full annual cycle distribution and population trends with citizen science data. *Ecological Applications*, 30(3). <https://doi.org/10.1002/EAP.2056>
- Fink, D., Hochachka, W. M., Zuckerberg, B., Winkler, D. W., Shaby, B., Munson, M. A., Hooker, G., Riedewald, M., Sheldon, D., & Kelling, S. (2010). Spatiotemporal exploratory models for broad-scale survey data. *Ecological Applications*, 20(8), 2131–2147. <https://doi.org/10.1890/09-1340.1>
- Forbes, M. G., & Dunton, K. H. (2006). Response of a subtropical estuarine marsh to local climatic change in the southwestern Gulf of Mexico. *Estuaries and Coasts*, 29(6), 1242–1254. <https://doi.org/10.1007/BF02781824>
- Formoso-Freire, V., Barbosa, A. M., Baselga, A., & Gómez-Rodríguez, C. (2023). Predicting the spatio-temporal pattern of range expansion under lack of equilibrium with climate. *Biological Conservation*, 288. <https://doi.org/10.1016/j.biocon.2023.110361>
- Gallardo, J. C., Macias, V., & Velarde, E. (2009). Birds (Vertebrata: Aves) of the Gulf of Mexico. *Gulf of Mexico--Origins, Waters, and Biota*, 1321–1342.
- Greenberg, R., Maldonado, J. E., Droege, S., & McDonald, M. V. (2006). Tidal Marshes: A Global Perspective on the Evolution and Conservation of Their Terrestrial Vertebrates. *BioScience*, 56(8), 675–685. [https://doi.org/10.1641/0006-3568\(2006\)56\[675:TMAGPO\]2.0.CO;2](https://doi.org/10.1641/0006-3568(2006)56[675:TMAGPO]2.0.CO;2)
- Haas, E. K., La Sorte, F. A., McCaslin, H. M., Belotti, M. C. T. D., & Horton, K. G. (2022). The correlation between eBird community science and weather surveillance radar-based estimates of migration phenology. *Global Ecology and Biogeography*, 31(11), 2219–2230. <https://doi.org/10.1111/geb.13567>
- Hirn, J., Sanz, V., García, J. E., Goberna, M., Montesinos-Navarro, A., Navarro-Cano, J. A., Sánchez-Martín, R., Valiente-Banuet, A., & Verdú, M. (2024). Transfer learning of

- species co-occurrence patterns between plant communities. *Ecological Informatics*, 83. <https://doi.org/10.1016/j.ecoinf.2024.102826>
- Jiménez-Valverde, A., & Lobo, J. M. (2007). Threshold criteria for conversion of probability of species presence to either-or presence-absence. *Acta Oecologica*, 31(3), 361–369. <https://doi.org/10.1016/j.actao.2007.02.001>
- Johnston, A., Auer, T., Fink, D., Strimas-Mackey, M., Iliff, M., Rosenberg, K. V., Brown, S., Lanctot, R., Rodewald, A. D., & Kelling, S. (2020). Comparing abundance distributions and range maps in spatial conservation planning for migratory species. *Ecological Applications*, 30(3). <https://doi.org/10.1002/eap.2058>
- Kingma, D. P., & Welling, M. (2022). *Auto-Encoding Variational Bayes*. <http://arxiv.org/abs/1312.6114>
- Klingbeil, B. T., Cohen, J. B., Correll, M. D., Field, C. R., Hodgman, T. P., Kovach, A. I., Lentz, E. E., Olsen, B. J., Shriver, W. G., Wiest, W. A., & Elphick, C. S. (2021). High uncertainty over the future of tidal marsh birds under current sea-level rise projections. *Biodiversity and Conservation*, 30(2), 431–443. <https://doi.org/10.1007/s10531-020-02098-z>
- La Sorte, F. A., Fink, D., Blancher, P. J., Rodewald, A. D., Ruiz-Gutierrez, V., Rosenberg, K. V., Hochachka, W. M., Verburg, P. H., & Kelling, S. (2017). Global change and the distributional dynamics of migratory bird populations wintering in Central America. *Global Change Biology*, 23(12), 5284–5296. <https://doi.org/10.1111/gcb.13794>
- Lesaffre, E., & Molenberghs, G. (1991). Multivariate probit analysis: A neglected procedure in medical statistics. *Statistics in Medicine*, 10(9), 1391–1403. <https://doi.org/10.1002/sim.4780100907>
- Li, L., Cole, S., Rodriguez-Flores, J. M., Hestir, E., Fink, D., Viers, J. H., Medellin-Azuara, J., Conklin, M., & Harmon, T. (2025). Synergies Between Agricultural Production and Shorebird Conservation With Climate Change in the Central Valley, California, With Optimized Water Allocation and Multi-Benefit Land Use. *Global Change Biology*, 31(6). <https://doi.org/10.1111/gcb.70304>
- Michener, W. K., Blood, E. R., Bildstein, K. L., Brinson, M. M., & Gardner, L. R. (1997). Climate change, hurricanes and tropical storms, and rising sea level in coastal wetlands. *Ecological Applications*, 7(3), 770–801.
- Norberg, A., Abrego, N., Blanchet, F. G., Adler, F. R., Anderson, B. J., Anttila, J., Araújo, M. B., Dallas, T., Dunson, D., Elith, J., Foster, S. D., Fox, R., Franklin, J., Godsoe, W., Guisan, A., O'Hara, B., Hill, N. A., Holt, R. D., Hui, F. K. C., ... Ovaskainen, O. (2019). A comprehensive evaluation of predictive performance of 33 species distribution models at species and community levels. *Ecological Monographs*, 89(3), 1–24. <https://doi.org/10.1002/ecm.1370>
- O'Neill, B. C., Tebaldi, C., Van Vuuren, D. P., Eyring, V., Friedlingstein, P., Hurtt, G., Knutti, R., Kriegler, E., Lamarque, J. F., Lowe, J., Meehl, G. A., Moss, R., Riahi, K., & Sanderson, B. M. (2016). The Scenario Model Intercomparison Project (ScenarioMIP) for CMIP6. *Geoscientific Model Development*, 9(9), 3461–3482. <https://doi.org/10.5194/gmd-9-3461-2016>
- Ovaskainen, O., Tikhonov, G., Norberg, A., Guillaume Blanchet, F., Duan, L., Dunson, D., Roslin, T., & Abrego, N. (2017). How to make more out of community data? A conceptual framework and its implementation as models and software. *Ecology Letters*, 20(5), 561–576. <https://doi.org/10.1111/ele.12757>

- Pierce, D. W., Kalansky, J. F., & Cayan, D. R. (2018). Climate, drought, and sea level rise scenarios for the Fourth California Climate Assessment. *California's Fourth Climate Change Assessment. Publication Number: CNRA-CEC-2018-006.*, August 2018, 71. www.climateassessment.ca.gov.
- Qian, X., Liu, L., Chen, X., Zhang, X., Chen, S., & Sun, Q. (2023). Global Leaf Chlorophyll Content Dataset (GLCC) from 2003–2012 to 2018–2020 Derived from MERIS and OLCI Satellite Data: Algorithm and Validation. *Remote Sensing*, 15(3). <https://doi.org/10.3390/rs15030700>
- Redding, D. W., Lucas, T. C. D., Blackburn, T. M., & Jones, K. E. (2017). Evaluating Bayesian spatial methods for modelling species distributions with clumped and restricted occurrence data. *PLoS ONE*, 12(11). <https://doi.org/10.1371/journal.pone.0187602>
- Ruiz-Gutierrez, V., Bjerre, E. R., Otto, M. C., Zimmerman, G. S., Millsap, B. A., Fink, D., Stuber, E. F., Strimas-Mackey, M., & Robinson, O. J. (2021). A pathway for citizen science data to inform policy: A case study using eBird data for defining low-risk collision areas for wind energy development. *Journal of Applied Ecology*, 58(6), 1104–1111. <https://doi.org/10.1111/1365-2664.13870>
- Rush, S. A., Soehren, E. C., Stodola, K. W., Woodrey, M. S., & Cooper, R. J. (2009). Influence of Tidal Height on Detection of Breeding Marsh Birds Along the Northern Gulf of Mexico. *The Wilson Journal of Ornithology*, 121(2), 399–405. <https://doi.org/10.1676/08-096.1>
- Soriano-Redondo, A., Jones-Todd, C. M., Bearhop, S., Hilton, G. M., Lock, L., Stanbury, A., Votier, S. C., & Illian, J. B. (2019). Understanding species distribution in dynamic populations: a new approach using spatio-temporal point process models. *Ecography*, 42(6), 1092–1102. <https://doi.org/10.1111/ecog.03771>
- Sullivan, B. L., Wood, C. L., Iliff, M. J., Bonney, R. E., Fink, D., & Kelling, S. (2009). eBird: A citizen-based bird observation network in the biological sciences. *Biological Conservation*, 142(10), 2282–2292. <https://doi.org/10.1016/J.BIOCON.2009.05.006>
- Suzuki, M., Nakayama, K., & Matsuo, Y. (2016). *Joint Multimodal Learning with Deep Generative Models*. <http://arxiv.org/abs/1611.01891>
- Tang, L., Xue, Y., Chen, D., & Gomes, C. P. (2018). *Multi-Entity Dependence Learning with Rich Context via Conditional Variational Auto-Encoder*. www.aaai.org
- Tobias, J. A., Sheard, C., Pigot, A. L., Devenish, A. J. M., Yang, J., Sayol, F., Neate-Clegg, M. H. C., Aloravainen, N., Weeks, T. L., Barber, R. A., Walkden, P. A., MacGregor, H. E. A., Jones, S. E. I., Vincent, C., Phillips, A. G., Marples, N. M., Montaña-Centellas, F. A., Leandro-Silva, V., Claramunt, S., ... Schleuning, M. (2022). AVONET: morphological, ecological and geographical data for all birds. *Ecology Letters*, 25(3), 581–597. <https://doi.org/10.1111/ele.13898>
- Van De Pol, M., Ens, B. J., Heg, D., Brouwer, L., Krol, J., Maier, M., Exo, K., Oosterbeek, K., Lok, T., Eising, C. M., & Koffijberg, K. (2010). Do changes in the frequency, magnitude and timing of extreme climatic events threaten the population viability of coastal birds? *Journal of Applied Ecology*, 47(4), 720–730. <https://doi.org/10.1111/j.1365-2664.2010.01842.x>
- Ward, E. J., Barnett, L. A. K., Anderson, S. C., Commander, C. J. C., & Essington, T. E. (2022). Incorporating non-stationary spatial variability into dynamic species

distribution models. *ICES Journal of Marine Science*, 79(9), 2422–2429.

<https://doi.org/10.1093/icesjms/fsac179>

Warton, D. I., Foster, S. D., De'ath, G., Stoklosa, J., & Dunstan, P. K. (2015). Model-based thinking for community ecology. *Plant Ecology*, 216(5), 669–682.

<https://doi.org/10.1007/s11258-014-0366-3>

Manuscript being submitted